Determination of the velocity of surface acoustic waves with excitation and detection by local electric field probes

A. Habib (1), U. Amjad (2), M. Pluta (2), U. Pietsch (1), and W. Grill (2)

(1) Department of Solid State Physics, University of Siegen, ENC, D-57072, Siegen, Germany
(2) Institute of Experimental Physics II, University of Leipzig, Linnéstr. 5, D-04103 Leipzig, Germany

PACS: 43.35.Pt, 43.35.Zc, 43.60.Lq, 43.35.Gk

ABSTRACT

In physical acoustics, visualization of individual acoustic wave fronts on piezoelectric crystal is one of the fundamental problems. Excitation of ultrasound in the Coulomb field of scanned electrically conductive spherical local probes and similar detection have been employed for imaging of the transport properties of acoustic waves in piezoelectric materials including single crystalline wafers. The excitation in the field of a local probe allows generation and detection of acoustic waves with a spatial resolution exceeding the diffraction limit. The temporal resolution is not limited by resonances as present in disc type transducers and periodically structured inter digital surface acoustic wave transducers. For generation and detection of surface acoustic waves two Coulomb probes have been positioned on a planar surface of piezoelectric crystals with one of the probes scanned in two dimensions to record spatial dependencies. Wide band operation as well as narrow band quadrature detection schemes has been applied for sensitive detection of the propagating waves. The method has been applied to image propagating surface acoustic waves in two dimensions. The generation and detection scheme as well as the numerical modeling are demonstrated and applications are exemplified.

INTRODUCTION

Sound waves in crystals depend on the fourth rank elastic constant tensor display a variety of anisotropic propagation phenomena. The direction in which the energy flows differs from the wave vector. Singularities for the energy transport can arise in the scenario addressed as "phonon focusing" in which the energy flow becomes very large, in fact infinite in the limit of geometric acoustics. Generation and detection of surface acoustic waves with digital and inter digital transducers (DT, IDT) attracted a large attention in the last several decades [1-10]. A series of experiments with different methods of wave field detection have already been performed such as by X-ray topography [4-6]. Later on wave front imaging has been achieved by scanning acoustic force electron microscopy [7], immersed focusing transducers [8] and by scanning electron microscopy methods [9].

Visualizing surface acoustic wave propagation in quartz and $LiNbO_3$ crystals started in the early 1980's [4]. The conventional way of generation and detection of surface acoustic wave (SAW) is normally based on DT or IDT which are fixed generating structure. This does not permit scanning of the wave vector in angle. In the experiments usually leaky longitudinal and surface acoustic waves are observed.

The main purpose of this paper is to utilize the inherent piezoelectric properties of a lithium niobate sample for transforming electrical signals into acoustic waves and vice versa. In order to describe the transport properties of acoustic waves in piezoelectric crystals, the customary procedure is to use the strain-induced stress and the electric-field-induced stress for the total stress in Newton's equation of motion for continuous media [11-13]. Since it is well known that the magnetic field has only a negligible effect in non-magnetic crystals, a quasi-static treatment is sufficient and, hence an electric potential may be introduced. That approach has already been presented in [14].

Experimental set up

A simplified experimental scheme of the transient acquisition is presented in figure 1. A similar experimental set-up for the Coulomb excitation and detection of surface acoustic waves has been reported previously [14]. An excitation burst with a carrier frequency of 89.9 MHz and duration of 220 ns (approximately, 20 oscillations) was cut by an electronic switch from a continuous sinusoidal signal (CW) generated by a stabilized oscillator. The electric burst signal is supplied to a sending point like electrode, where it is converted by the piezo-effect into ultrasound propagating in the piezoelectric sample of interest (figure 2). On the same side of the sample the ultrasonic oscillations are converted back into an electric signal by a receiving tip.

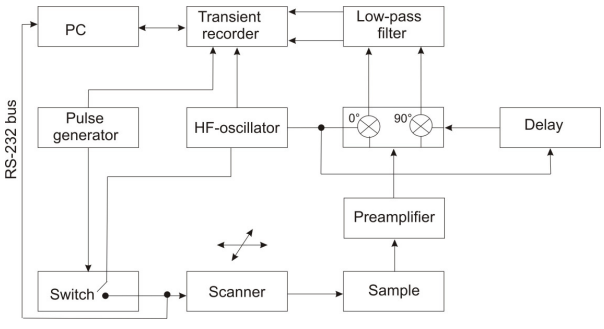

Figure 1: Schematic drawing of the signal generation, detection, and processing for the Coulomb excitation and detection. Scanner (sending electrode) is moving in xy direction.

A quadrature detection scheme is employed to the received signal. It is pre-amplified and supplied to two multipliers (figure 1). In the first channel the received signal is multiplied with the reference signal, and in the second channel it is multiplied with the reference CW signal, whose phase is shifted by 90° with the aid of a suitably adjusted cable length. After filtering out the high frequency components of the product signals, the low frequency components are acquired by a two channel 8-bit transient recorder.

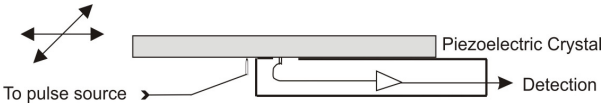

Figure 2: Schematic diagram for piezoelectric excitation and detection of ultrasound.

Two motor-driven translation stages were used to position the excitation probe in two dimensions on the surface of the sample. The scanning tips were manufactured from a 50 µm gold wire that was in contact with the sample and a 200 µm bronze supporting wire for the triangular lever for the excitation signal. The scanned contact was used for excitation. On the other hand a fixed probe manufactured from similar components as used for detecting the signal (figure 2). The scanner moved the probe across the sample surface, while the transferred electric signal transient was registered and averaged for each position. The typical scan area was 4×4 mm^2.

The transients of the 2 channels of the quadrature detection scheme are acquired with a sampling frequency equal to the ultrasonic signal frequency of 89.9 MHz, for each pixel, representing a third dimension of the acquired data.

The described data acquisition technique has already been used with conventional focusing ultrasound transducers [15]. As compared to the time-selective boxcar technique [16], it enables one to record multiple time delay images in one scan allowing variable gating of the recorded signal by processing of the stored data. An advantage of the above mentioned technique is, that a three-dimensional set of complex numbers can be acquired involving only a two-dimensional mechanical scan. This is achieved by the time resolved detection and allows a holographic registration of the propagation of surface acoustic waves and volume waves including signals resulting from leaky surface waves. The respective analysis is entirely performed by post-experimental processing of the acquired three-dimensional (position in two dimensions x, y, and time) data set.

Result and discussion

Figure 3 displays the magnitude of a transient, acquired at the corner of the scanned area (upper left in figure 4 and 5). In this experiment the sound wave packages were detected on the surface of a lithium niobate ($LiNbO_3$) single-crystal (5.02 mm thick, Y-Z oriented crystal disc, both sides polished). All images acquired for this experiment cover an area of 4×4 mm^2 of the crystal surface and about 10 µs length of the transient in time.

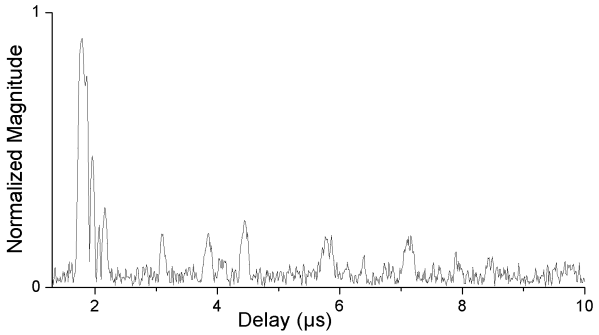

Figure 3: Transient recorded with point like source and recorded with same method on the same side of the excitation. For each position of the exciting electrode such a transient was recorded.

In figure 3, the first signal occurs at 1.66 µs, caused by an electrical cross talk. This cross talk represents the time of excitation (figure 3). The next signal (at about 3.07 µs) is caused by leaky longitudinal wave (figure 4). At about 3.85 µs the surface acoustic wave is observed (figure 5).

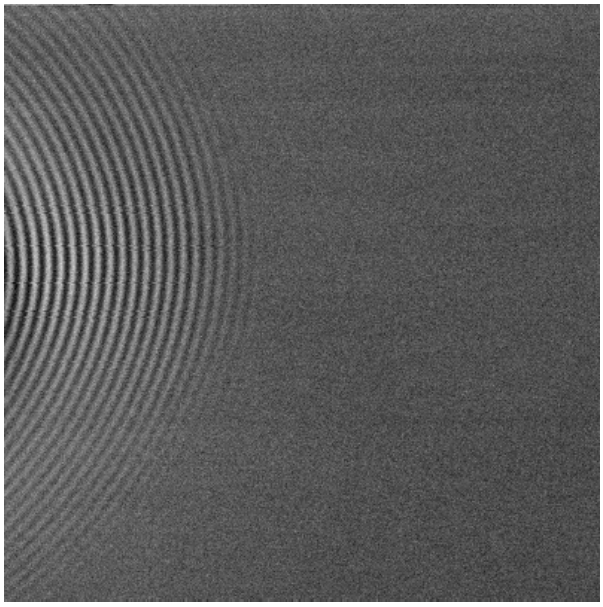

Figure 4: Scanned wave field of the leaky longitudinal wave. The contrast in the image is derived from the real part of the quadrature detection with medium grey representing zero. The width of the image is 4 mm. The contrast in the image represents the real (0° referenced) part of the quadrature detection with medium grey relating to zero.

It is well known that longitudinal waves have a higher sound velocity then the Rayleigh surface acoustic waves [17]. The surface acoustic waves are therefore trailing the longitudinal waves travelling along the surface. This is also visible in the recorded transient (figure 3) and can be compared with figure 4 and figure 5.

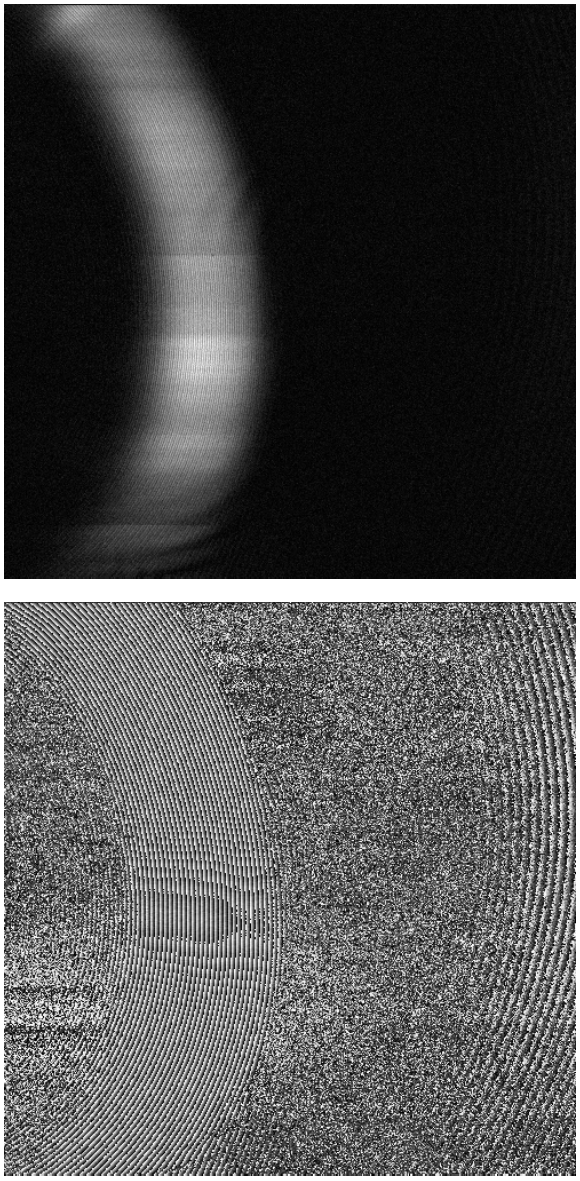

Figure 5: Scanned wave field of the surface acoustic waves. Image in magnitude contrast (top); and phase contrast with full grey scale equal to 2π (bottom). The width of the images is 4 mm.

The surface acoustic wave length (39.60 μm) was derived from the images. The source of the periodic contrast is the corrugation of the sample surface induced by SAW.

The value of SAW velocity obtained from the measurements, is c=3.56 (±0.06) km/s, in good agreement with values given in [17]. The measured leaky longitudinal wave velocity is 7.44 (±0.03) km/s.

The wave velocity determination

Wave field distribution (as represented in figure 4) is recorded with the application of the quadrature detection scheme, so the stored data array may be treated as samples of complex valued field $\psi(x, y, t)$, that may be superposed, at selected instant of time, from planar wave components of the type

$$\Psi(f_x, f_y)\exp[2\pi i(f_x x + f_y y)] \qquad (1)$$

For a wave running to the right (positive x axis) the Fourier amplitudes shall differ from zero only in the case $f_x > 0$. Fourier spectrum of the 2D quadrature detection measurements performed in the half space $x > 0$, (by assumption that $(0, 0)$ is the position of the source) is also asymmetric (see figure 6). In the figure 6, positions of maxima are related to the reciprocals of respective wavelengths or spatial frequencies (f_x, f_y). By sampling in space with step of $\Delta x = \Delta y = 0.01\,mm$, the Nyquist spatial frequency is 50 1/mm. While sampling of the wave field fulfils that sampling criteria (we were collecting about four points per the shortest wave cycle), it is not fulfilled for higher harmonics. On one hand that causes the aliasing effect, but on the other hand positions of higher harmonics maxima could still bring additional information on the observed velocities. That is why we show (figure 6) more than a basic square in the spatial frequency space (periodicity of the spectrum of sampled wave field is visible in such presentation).

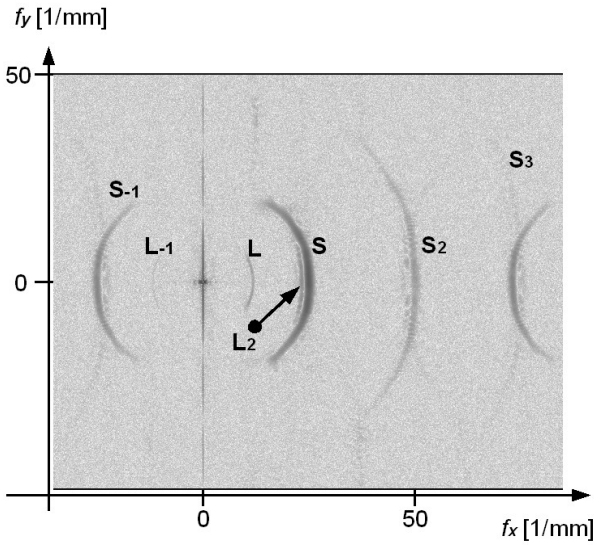

Figure 6: Two dimensional Fourier spectrum of registered complex valued field presented in negative logarithmic scale (maxima dark). L: spectrum of longitudinal wave, L_2: second order spectrum of longitudinal wave, L_{-1}: weak 1st order spectrum of the longitudinal wave. S, S_2 and S_3 respective orders of spectrum of the slower surface wave. S_{-1}: relatively strong 1st order spectrum of the slower wave. Due to the aliasing effect some maxima for spatial frequencies $f_x > 0$ overlap with maxima for $f_x < 0$.

Positions of the maxima in spectrum along f_x axis are presented in the table below. The respective wavelengths are calculated with the formula

$$\lambda = n / f_x \qquad (2)$$

where $n = -1, 1, 2, 3$ is the order of the observed maximum. The respective velocities are calculated as $c = \lambda f$, where $f = 89.9\,MHz$ is the frequency applied in the experiment. Uncertainty of the result (visible in the figure 6 as the finite width of the maxima) is related to the finite length of applied excitation pulse.

Table 1. Spatial frequencies, wavelength, and calculated velocities from the 2D Fourier spectrum of the wave field.

Type of wave	f_x [1/mm]	λ [μm]	c [km/s]
L	12.1	82.6	7.42
L_2	23.8	83.8	7.54
L_{-1}	-12.3	81.2	7.3
S	25.6	39.1	3.51
S_2	51.2	39.1	3.51
S_3	76.7	39.1	3.51
S_{-1}	-25.6	39.1	3.51

The surface acoustic wave velocity calculated here is slightly mismatched with the experimental value [Table 1]. A possible reason for the difference could be a minor mis-alignment of the crystal to the sample surface.

Conclusion

The results obtained in this paper demonstrate the potential of holographic imaging capability by means of Coulomb excitation and detection for the study of the electro-mechanical properties of piezoelectric materials. The method of excitation and detection is simple and versatile. It allows for variation of the frequency of the surface acoustic waves over a wide range since neither mechanical nor electrical resonances are involved in the coupling scheme. The experiments presented here have been performed on single-crystalline nearly Y-Z oriented lithium niobate single-crystal. For the first time surface acoustic waves (SAW) have been observed with the developed Coulomb excitation and detection scheme. The holograms shown in this paper will lead us for a suitable basis for the determination of phonon focusing. This Coulomb excitation and detection for SAW will find a new avenue in the field Rayleigh surface acoustic waves generation and detection as well as in the direction of phonon focusing.

Acknowledgements

The support of the European Union under the 7th Framework Programme within AISHA II (Aircraft Integrated Structural Health Assessment II) is gratefully acknowledged. A. Habib wishes to acknowledge support of DAAD (Deutscher Akademischer Austausch Dienst) by a travel grant and support provided by the University of Leipzig.

REFERENCES

1. R. M. White and F. W Voltmer, "Direct piezoelectric coupling to surface elastic waves" *App. Phy. Lett*, **7**, 314-316, (1965)
2. G. W. Farnell. “Properties of elastic surfaces waves”, W. P Mason and R. N. Thurston, eds, “Physical Acoustics”, Vol. 6, pp. 109–166, Academic Press, New York, (1970)
3. K. Yamanouchi, and K. Shibayama, “Propagation and amplification of Rayleigh waves and Piezoelectric leaky surface waves in $LiNbO_3$” *J. Appl. Phy*, **43**, 856-862, (1972)
4. R. W. Whatmore, P. A. Goddard, B. K. Tanner, and G. F. Clark , "Direct imaging of travelling Rayleigh waves by stroboscopic X-ray topography". *Nature*, 299. 44-46. (1982)
5. H. Cerva, and W. Graeff, "Contrast investigations of surface acoustic waves by stroboscopic topography. I. Orientation contrast". *Phys. Stat. Sol. (a)*, **82**. 35-45. (1984)
6. D. V. Roshchupkin, M. Brunel, R. Tucoulou, E. Bigler, and NG. Sorokin, “Reflection of surface acoustic waves on domain walls in a $LiNbO_3$ crystal". *App. Phy. Lett,* 64. 164-165. (1994)
7. T. Hesjedal, E. Chilla, and H.-J. Froehlich, "Scanning acoustic force microscope investigations of surface acoustic waves". *Surf. Interface Anal*, **25**. 569-572. (1997)
8. R. E Vines, Shin-ichiro Tamura, and J. P. Wolfe, "Surface acoustic wave focusing and induced Rayleigh waves". *Phys. Rev. Lett*, **74.** 2729-2732. (1995)
9. D. V. Roshchupkin, M. Brunel, R. Tucoulou, E. Bigler, and NG. Sorokin, “Reflection of surface acoustic waves on domain walls in a LiNbO3 crystal". *App. Phy. Lett*, **64**. 164-165. (1994)
10. J. P. Wolfe, "Acoustic wavefronts in crystalline solids". *Phys. Today*, 48. 34-40. (1995)
11. J. J. Kyame, “Wave propagation in piezoelectric crystals”, *J. Acoust. Soc. Am*. **21**, 159-167, (1949)
12. I. Koga, M. Aruga, and Y. Yoshinaka, “Theory of plane elastic waves in a piezoelectric crystalline medium and determination of elastic and piezoelectric constant of quartz”, *Phys. Rev*. **109**, 1467-1473, (1958)
13. H. F. Tiersten, “Thickness vibrations of piezoelectric plates”, *J. Acoust. Soc. Am*. **35**, 53-58, (1963)
14. A. Habib, E. Twerdowski, M. von Buttlar, M. Pluta, M. Schmachtl, R. Wannemacher and W. Grill. "Acoustic holography of piezoelectric materials by Coulomb excitation". in Proc. SPIE. 6177, **61771A**, (2006)
15. E. Twerdowski, R. Wannemacher, N. Razek, A. Schindler, and W. Grill "Application of spatially and temporally apodized non-confocal acoustic transmission microscopy to imaging of directly bonded wafers" *Ultrasonics* **44**, 54-63, (2006)
16. W. Grill, K. Hillmann, K. U. Würz, and J. Wesner, “Scanning ultrasonic microscopy with phase contrast”, “Advances in acoustic microscopy”, A. Briggs and W. Arnold, eds., vol. 2, (Plenum Press, New York, 1996) pp. 167-217
17. SG. Joshi, BD. Zaitsev, IE. Kuznetsova, AA. Teplykh, A. Pasachhe, “Characteristics of fundamental acoustic wave modes in thin piezoelectric plates” *Ultrasonics* **44**, 787-791, (2006)